A Novel Method to Minimize Torque Ripple, Mechanical Vibration, and Noise in a Direct Torque Controlled Permanent Magnet Synchronous Motor Drive

Arumugam Sivaprakasam
Kongu Engineering College, Perundurai, Erode, Tamil Nadu, India, 638052

Thathan Manigandan
P.A.College of Engineering and Technology, Pollachi, Tamil Nadu, India

(Received 28 March 2013; accepted 3 March 2014)

The Direct Torque Control (DTC) technique of the Permanent Magnet Synchronous Motor (PMSM) receives increasing attention due to its simplicity and robust dynamic response compared with other control techniques. The classical switching table based DTC presents large flux, torque ripples, and more mechanical vibrations in the motor. Several studies have been reported in the literature on classical DTC. However, only limited studies exist that actually discuss or evaluate the classical DTC. This paper proposes a simple DTC method/switching table for PMSM, to reduce flux and torque ripples as well as mechanical vibrations and noise. In this paper, two DTC schemes are proposed. The six sector and twelve sector methodology is considered in DTC Scheme I and DTC Scheme II, respectively. In both DTC schemes, a simple modification is made in the classical DTC structure by eliminating the two-level inverter available in the classical DTC and replacing it with a three-level Neutral Point Clamped (NPC) inverter. To further improve the performance of the proposed DTC Scheme I, the available 27 voltage vectors are allowed to form different groups of voltage vectors such as Large-Zero (LZ), Medium-Zero (MZ), and Small-Zero (SZ), whereas in DTC Scheme II, all the voltage vectors are considered to form a switching table. Based on these groups, a new switching table is proposed. The proposed DTC schemes are comparatively investigated with the classical DTC and existing literatures from the aspects of theory analysis and computer simulations. It can be observed that the proposed techniques can significantly reduce the flux, torque ripples, mechanical vibrations, and noise and improve the quality of current waveform compared with traditional and existing methods.

1. INTRODUCTION

Around 40 years ago, in 1972, Blaschke proposed the concept of Field Oriented Control (FOC) for Induction Motor.[1] Since then, the FOC dominates in the advanced AC drive market, even though it has a complicated structure. Thirteen years later, a new control technique for the Torque Control of Induction Motor was proposed by Takahashi and Noguchi as Direct Torque Control (DTC).[2] Two years later, Depenbrock presented another one control technique named Direct Self Control (DSC).[3] The first follows circular trajectory, and later follows hexagon trajectory. Both of them proved that it is possible to obtain a good dynamic control of the torque without any sensor on the mechanical shaft. Thus, DTC and DSC can be considered a sensorless type control technique.

The DTC scheme is normally preferred for low and medium power applications, whereas the DSC scheme is preferred for high power applications. In this paper, attention is focused on the DTC scheme, which is best suited for low and medium power applications. DTC overcomes the drawbacks of FOC such as the requirement of current regulators, co-ordinate transformations, and PWM signal generators. DTC also provides high efficiency, high power/torque density, and high reliability. Due to its simplicity, DTC allows a good torque control in steady states and start-up transient states.

In recent years, DTC has been popular for a variety of electrical machines. In 1997, Zhong et al. proposed the concept of DTC for PMSM.[4] Some of the researchers proposed this technique for Synchronous Reluctance Machines.[5] On the other hand, the classical DTC has some disadvantages and major disadvantages are as follows:

1) Difficulty to control torque at very low speed;

2) High current/torque ripple;

3) More mechanical vibrations.

Most of the literature surveyed has analysed classical DTC using two-level inverters, and all have presented a high degree of torque ripple in the results under dynamic conditions; this will reflect in the speed and current too.[6–10] In this paper, the possibilities for minimization of torque ripple and mechanical vibration in DTC is focused. The minimization of torque ripple is achieved by improvements in the areas such as inverters and switching tables.

In this paper, the conventional two-level inverter is replaced by the three-level Neutral Point Clamped (NPC) inverter which will have 27 voltage vectors, where only 8 voltage vectors are available with the classical DTC. The 27 voltage vectors that include large and medium voltage vectors have six numbers each, small voltage vectors have twelve numbers and three numbers of zero voltage vectors.

Some of the literature presents a three-level inverter with a classical DTC, but it utilizes all of the 27 voltage vectors to construct the switching table.[11–16] This paper proposes three kinds of DTC schemes to reduce torque ripple and mechanical vibrations. In the DTC Scheme I, only any two voltage vectors (large-zero or medium-zero or small-zero) alone are utilized to construct a switching table. All the voltage vectors are considered to form a switching table in DTC Scheme II.

Thus on the basis of the experience of the authors, the fair comparison between all the schemes are presented in both steady state and start-up transient state conditions. The comparison is useful to indicate to the users which one of the schemes can be effectively utilized today for various applications that require torque control.

2. MODEL OF PMSM

2.1. Machine Equations

The mathematical model of a PMSM can be expressed as

$$U_\alpha = -\frac{1}{\sqrt{3}}U_{ys} + \frac{1}{\sqrt{3}}U_{bs}; \tag{1}$$

$$U_\beta = \frac{2}{3}U_{rs} - \frac{1}{3}U_{ys} - \frac{1}{3}U_{bs}; \tag{2}$$

and the stator flux equations are

$$\varphi_{\alpha s} = \int (U_\alpha - R_s i_\alpha)\, dt; \tag{3}$$

$$\varphi_{\beta s} = \int (U_\beta - R_s i_\beta)\, dt; \tag{4}$$

$$|\varphi_s| = \sqrt{\varphi_{\alpha s}^2 + \varphi_{\beta s}^2}; \tag{5}$$

and the electromagnetic torque developed by a PMSM in a stationary reference frame is expressed as:[17]

$$T_e = \frac{3}{2}p\left(\varphi_s \times i_s\right); \tag{6}$$

or

$$T_e = \frac{3}{2}p\left(i_\beta \varphi_{\alpha s} - i_\alpha \varphi_{\beta s}\right). \tag{7}$$

2.2. Voltage Vector Impact on Torque

According to the principle of DTC, an electrical angle between stator and rotor flux vectors, δ can control the torque developed by the PMSM. This can be achieved by controlling the voltage vector. Hence, the voltage vector is the prime controllable input variable in DTC. However, it is mandatory to develop a relationship between the torque developed and the voltage vector.

The voltage and stator flux equations in stationary frame are expressed as

$$U_s = \frac{d\varphi_s}{dt} + R_s i_s \tag{8}$$

and

$$\varphi_s = L_s i_s + \varphi_r. \tag{9}$$

From Eqs. (8) and (9), we can get

$$L_s \frac{di_s}{dt} = U_s - R_s i_s - \frac{d\varphi_r}{dt} \tag{10}$$

and

$$L_s \frac{di_s}{dt} = U_s - R_s i_s - j\omega\varphi_r. \tag{11}$$

From Eq. (6), the torque differentiation with respect to time t is

$$\frac{dT_e}{dt} = \frac{3}{2}p\left\{\left(\frac{d\varphi_s}{dt} \times i_s\right) + \left(\frac{di_s}{dt} \times \varphi_s\right)\right\}; \tag{12}$$

Substituting Eqs. (8), (9), and (11) in (12), we can get

$$L_s \frac{dT_e}{dt} = \frac{3}{2}p\varphi_r \times U_s - \frac{3}{2}p\omega\varphi_r \cdot \varphi_s - R_s T_e \tag{13}$$

and

$$L_s \frac{dT_e}{dt} = T_{e\mathrm{I}} + T_{e\mathrm{II}} + T_{e\mathrm{III}}. \tag{14}$$

It can be seen from Eq. (13) that the equation contains three components.[15,18] The second component is negative and a function of speed. The third component is also negative and depends on stator resistance. The first component is always positive and depends on the voltage vector. From this, it is concluded that the non-zero vector always increases the torque developed, and the zero vectors always decrease the torque developed.

3. CLASSICAL DTC METHOD

Based on the errors between the reference and the actual values of torque and flux, it is possible to directly control the inverter switching states in order to reduce the torque and flux errors within the prefixed band limits. That is why this technique is called Direct Torque Control.[19–23] The block diagram of the classical DTC for PMSM is shown in Fig. 1.

The basic principle of DTC is to select stator voltage vectors according to the differences between the reference and actual torques. The reference and actual value of the stator flux is processed through a two-level hysteresis comparator. If the error is positive, the magnitude of the flux has to be increased, and this is denoted as $d\varphi_s = 1$. If the error is negative, the magnitude of the flux has to be decreased, and this is denoted as $d\varphi_s = 0$. The flux comparator conditions are given as,

$$d\varphi_s = 1 \quad \text{for} \quad |\varphi_s| \leq |\varphi_{s\mathrm{ref}}| - |\Delta\varphi_s| \tag{15}$$

and

$$d\varphi_s = 0 \quad \text{for} \quad |\varphi_s| \geq |\varphi_{s\mathrm{ref}}| + |\Delta\varphi_s|. \tag{16}$$

The rotor reference speed is compared with the actual rotor speed, and the error obtained is converted into reference torque by using a suitable PI regulator.[23–26]

The reference and actual torque is processed through a three-level hysteresis comparator. If the error is positive, the magnitude of torque has to be increased, and this is denoted as $dT_e = 1$. If the error is negative, the magnitude of torque has to be decreased, and this is denoted as $dT_e = -1$. If the error is zero, the magnitude of torque has to be maintained constant,

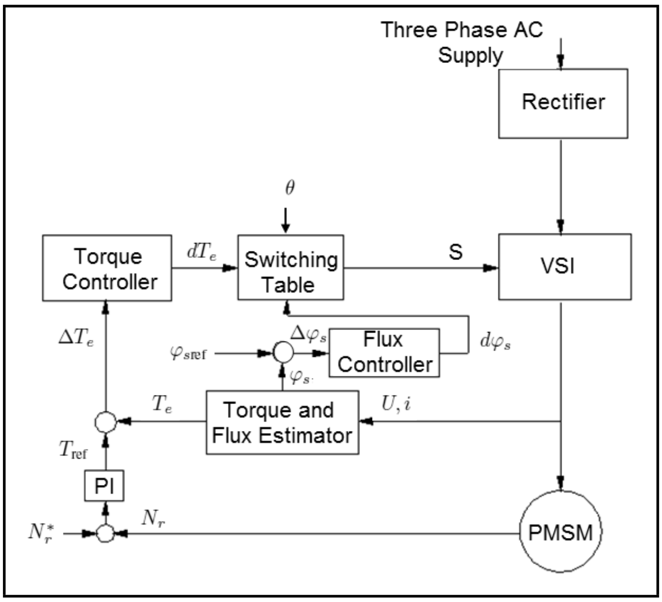

Figure 1. Block diagram of the classical DTC.

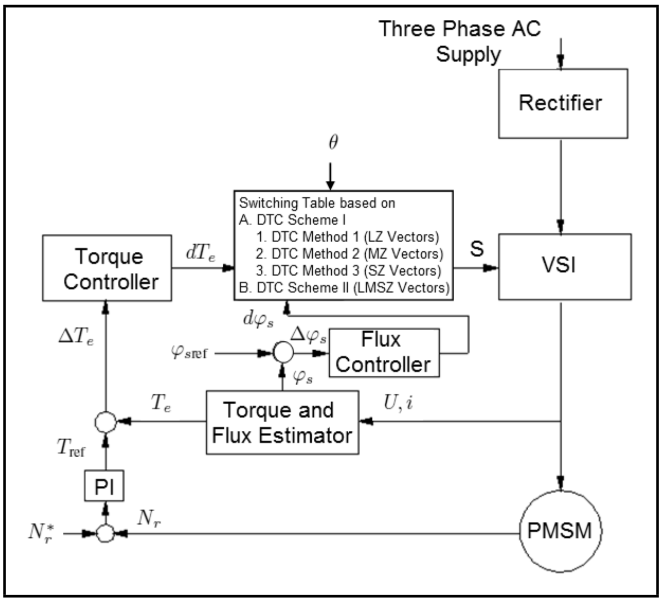

Figure 2. Block diagram of the proposed DTC schemes.

and this is denoted as $dT_e = 0$. The torque comparator conditions are given as,

$$dT_e = 1 \quad \text{for} \quad |T_e| \leq |T_{\text{ref}}| - |\Delta T_e|; \tag{17}$$

$$dT_e = -1 \quad \text{for} \quad |T_e| \geq |T_{\text{ref}}| + |\Delta T_e|; \tag{18}$$

and

$$dT_e = 0 \quad \text{for} \quad |T_{\text{ref}}| - |\Delta T_e| \leq |T_e| \leq |T_{\text{ref}}| + |\Delta T_e|. \tag{19}$$

Finally, the most suitable voltage vectors are selected form the switching table based on the flux and torque errors for all the sectors.[27–30]

4. PROPOSED DTC METHOD

The classical DTC uses a two-level inverter and produces only eight voltage vectors which includes six numbers of non-zero vectors, and the rest of them are zero vectors. This does not allow smooth variation in the flux and torque. This could be one of the main reasons for large flux, torque ripples, and mechanical vibrations. In this proposed DTC method, the two-level inverter is replaced by the NPC three-level inverter. Due to increment in the level of the inverter, there are 27 voltage vectors available to construct the switching table, which includes six numbers of large vectors, twelve numbers of small vectors, three numbers of zero vectors, and the remaining are medium vectors. The inference from Section 3 is that the switching table plays an important role in the DTC technique. For a proper switching table, the best result can be obtained. The structure of the proposed DTC schemes is shown in Fig. 2. In the proposed DTC Scheme I, the available 27 voltage vectors are allowed to form different groups of voltage vectors such as Large-Zero (LZ), Medium-Zero (MZ), and Small-Zero (SZ). Based on these groups, a new switching table is proposed. In the proposed DTC Scheme II, all the voltage vectors are considered for a switching table. The proposed DTC methods provide satisfactory results as compared to classical DTC. Table 1 provides the technical idea of the proposed DTC schemes.

Table 1. Technical difference among the classical and proposed DTC schemes.

Techniques used	Classical DTC	Proposed DTC Scheme I			Proposed DTC Scheme II
		DTC method 1	DTC method 2	DTC method 3	DTC method 4
Number of Sectors used	Six	Six	Six	Six	Twelve
Inverter Level	Two	Three	Three	Three	Three
Nature of Voltage Vectors used	LZ	LZ	MZ	SZ	LMSZ

4.1. Proposed DTC Scheme I

The proposed DTC Scheme I includes DTC method 1, DTC method 2, and DTC method 3, and all follow the six sector methodology.

4.1.1. DTC method 1

The proposed DTC method 1 utilizes large and zero voltage vectors. In this method, nine voltage vectors are used, in which six of them are large voltage vectors, and three of them are zero voltage vectors. This method is almost an imitation of the classical DTC because, in both cases, only large and zero voltage vectors are used. The switching table is constructed using these nine voltage vectors. The switching table developed in this method is almost similar to the classical DTC switching table. The drawback obtained in the DTC is repeated in this method also because of the non-availability of intermediate voltage vectors.

4.1.2. DTC method 2

In the proposed DTC method 2, the medium and zero voltage vectors are used to construct the switching table. There are six medium voltage vectors and three zero voltage vectors available. In DTC method 1, the large and zero voltage vectors are used; that means the switching is between large voltage vectors and zero voltage vectors. This will produce large ripples in the flux and torque. However, in DTC method 2, the

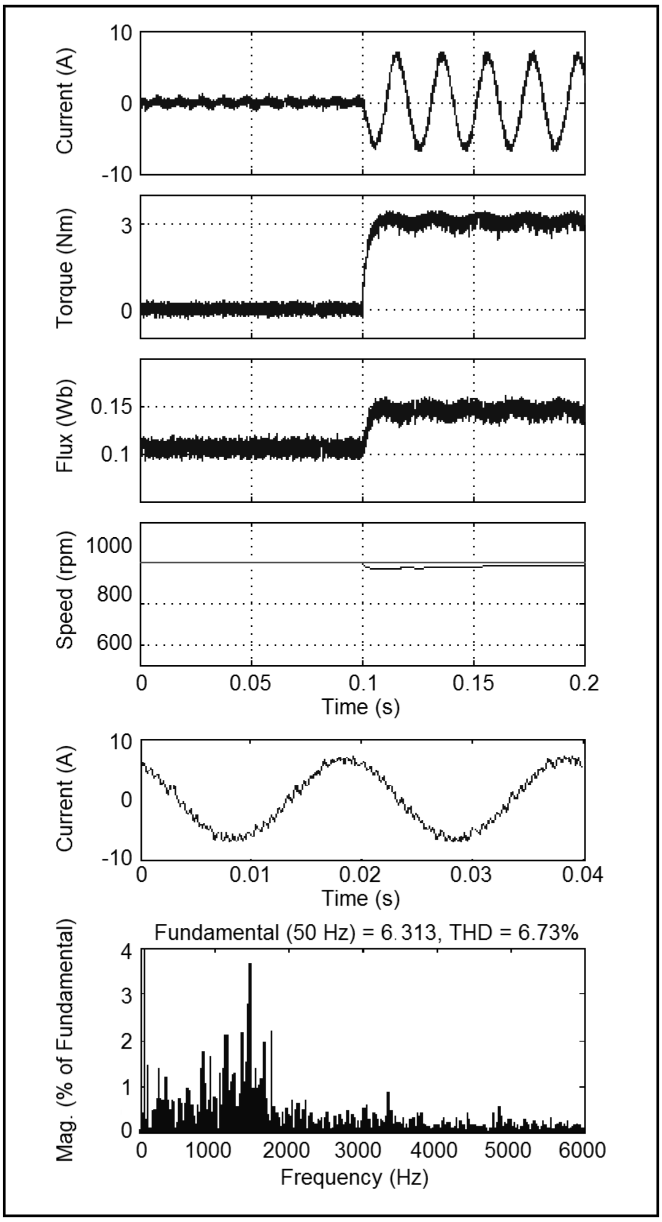

Figure 3. Response of classical DTC at 1000 rpm with an external load of 3 Nm.

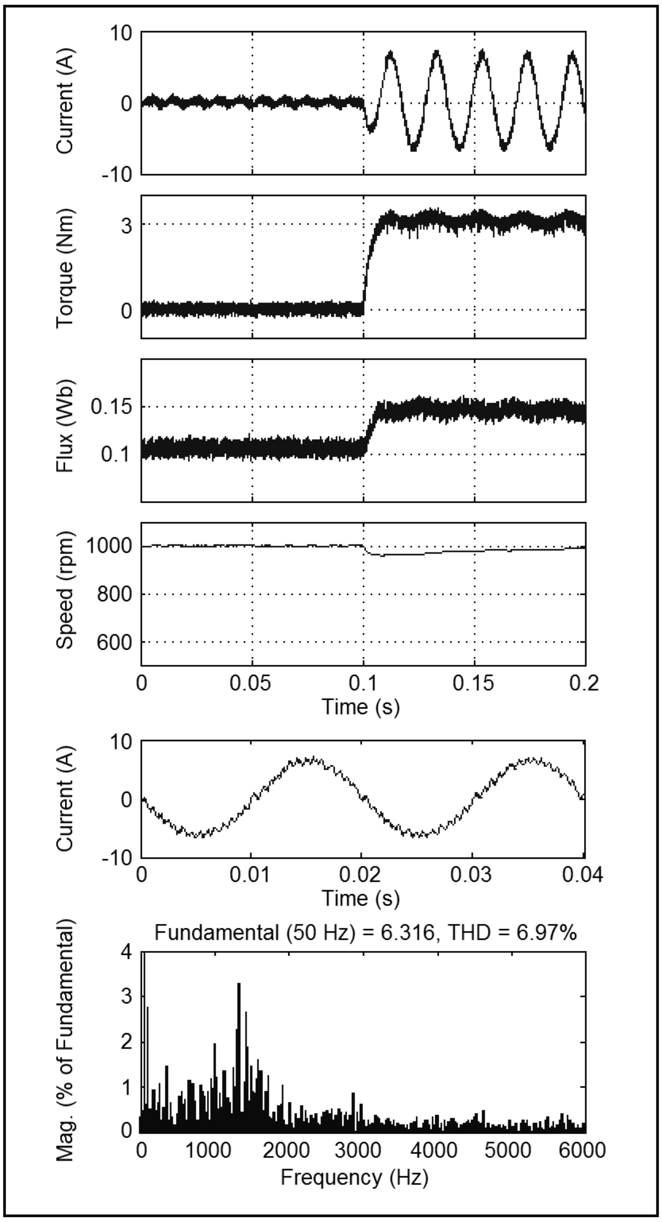

Figure 4. Response of DTC method 1 at 1000 rpm with an external load of 3 Nm.

medium and zero voltage vectors are used, so the ripples in the flux and torque are considerably reduced as compared to DTC method 1. This can be observed from Fig. 8 through Fig. 12.

4.1.3. DTC method 3

The DTC method 2 produces slightly lesser torque ripples as compared to the classical DTC method. This is because of no large voltage vectors are used in this method. From the experience of previous methods, the switching of the vector plays important role in the flux and torque ripple reduction. The switching from zero voltage to large/medium voltage increases the ripples in the flux and torque, harmonic content, and stress across the switching devices.

To overcome these problems, an appropriate switching table is constructed using only small and zero voltage vectors. Equation (13) tells us that the large voltage vectors contribute to a torque in the same direction, which will lead to large errors in the actual torque. This is true for small voltage vectors also. The lesser torque ripples can be expected by combining small and zero voltage vectors. There are twelve small voltage vectors and three zero voltage vectors available in this method. The small voltage vector exists in a redundant pair (i.e., six positive small vectors and six negative small vectors). So, the switching table is formed either by using a positive small vector or a negative small vector in order to balance neutral point potential. The small voltage vectors are selected to meet the demand of the flux and torque, as well as to reduce the flux, torque ripples, and mechanical vibrations. So, this ensures the safe operation of the entire system.

4.2. Proposed DTC Scheme II

The proposed DTC Scheme II is different in the view of the number of sectors used and the techniques used in the switching table formation. In this scheme, all the voltage vectors are used to form the switching table. This is referred to as DTC method 4 in the future.

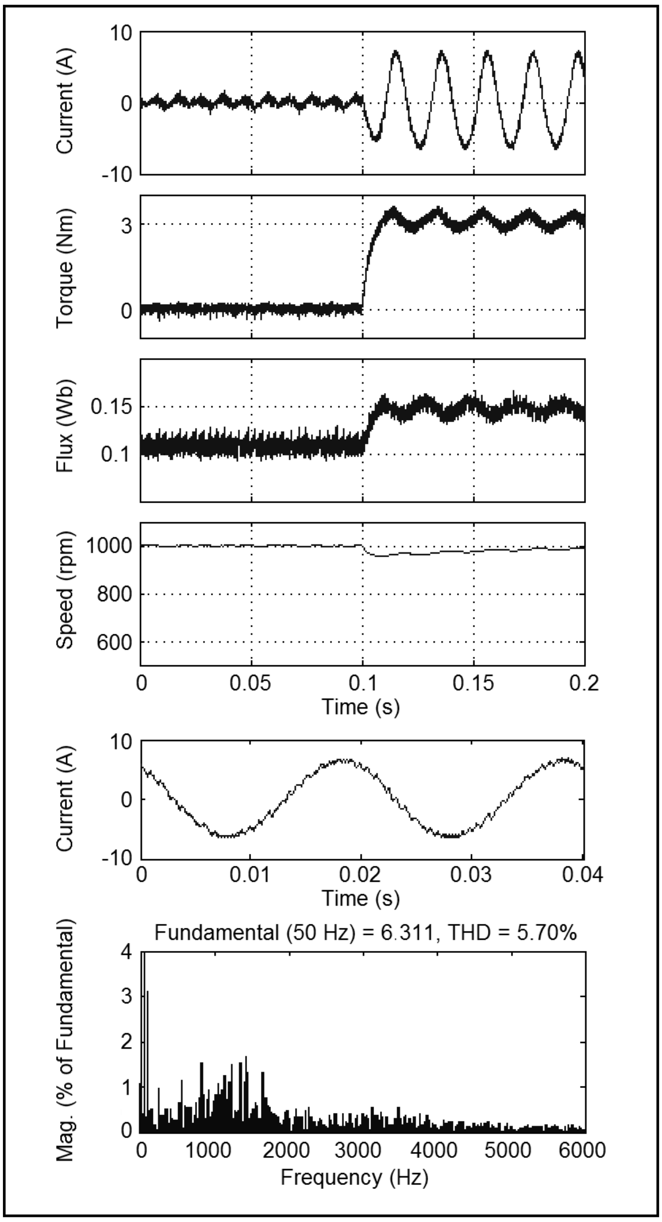

Figure 5. Response of DTC method 2 at 1000 rpm with an external load of 3 Nm.

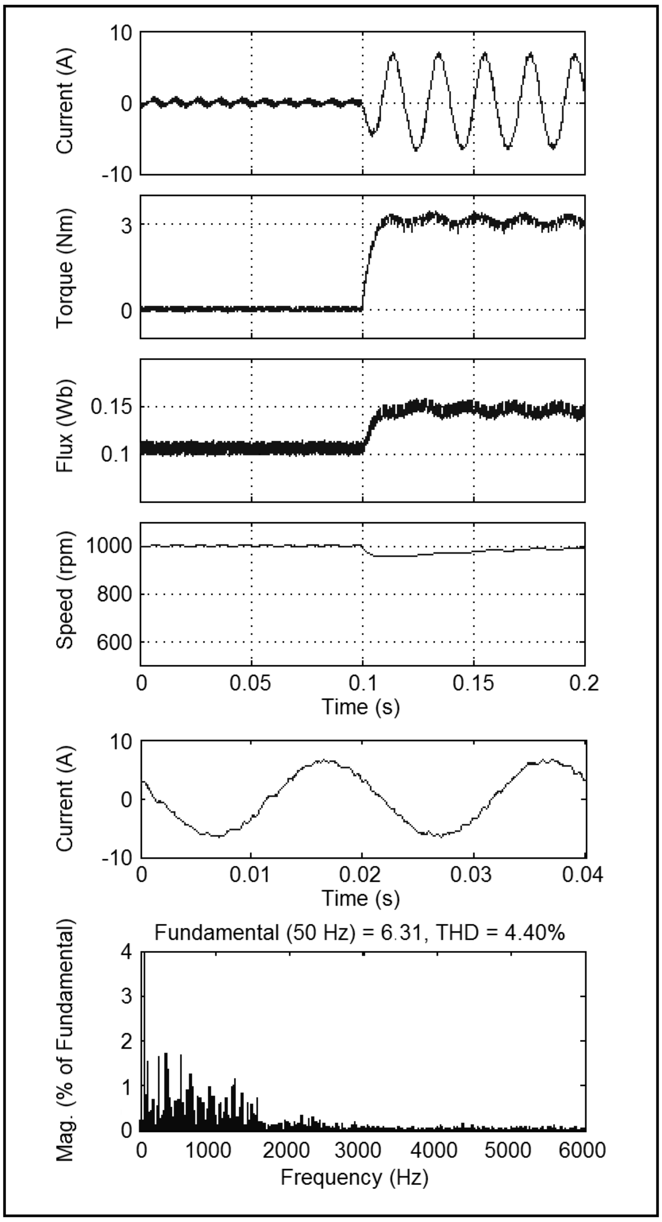

Figure 6. Response of DTC method 3 at 1000 rpm with an external load of 3 Nm.

5. SIMULATION AND RESULTS

The MATLAB/Simulink is used to perform the simulation for the proposed DTC methods and classical DTC method. The machine parameters used in this paper are the same as in two recent publications of Zhang and Zhu.[13,14] In this paper, the simulation results of classical DTC, DTC method 1, DTC method 2, DTC method 3, and DTC method 4 were presented. For all the methods, the performance analysis was carried out in different points of view such as performance at different operating points and performance during external load disturbance.

5.1. Comparative Study with Existing Work

First, the classical DTC was carried out to show the effectiveness of the proposed DTC methods. The proposed methods are also compared with existing works of Zhang and Zhu.[13,14] The switching table used in Fig. 2 is different from the literature.[13,14]

Figures 3 to 7 present the responses at 1000 rpm with an external load of 3 Nm applied at 0.1 s for classical DTC, DTC method 1, DTC method 2, DTC method 3, and DTC method 4. From the top to bottom, the waveforms are stator current, torque, flux, rotor speed, and the harmonic analysis of stator current, respectively. It can be seen that the current waveform is more sinusoidal in the proposed DTC methods as compared to existing methods. The classical DTC exhibits large flux and torque ripples. The Total Harmonic Distortion (THD) is calculated up to 6000 Hz.

The quantitative results are carried out at 1000 rpm with a 3 Nm external load for all the methods. It is seen that the stator current THD of the proposed DTC method 3 is 4.40%, much lower than the 5.85% and 4.67% of the existing DTC methods available in the paper Zhang and Zhu[13] and Zhang and Zhu,[14] respectively. The DTC method 4 provides lesser stator current THD as compared to classical DTC and reference Zhang and Zhu.[13] Among all the proposed DTC methods and existing DTC methods, the DTC method 3 provides better performance

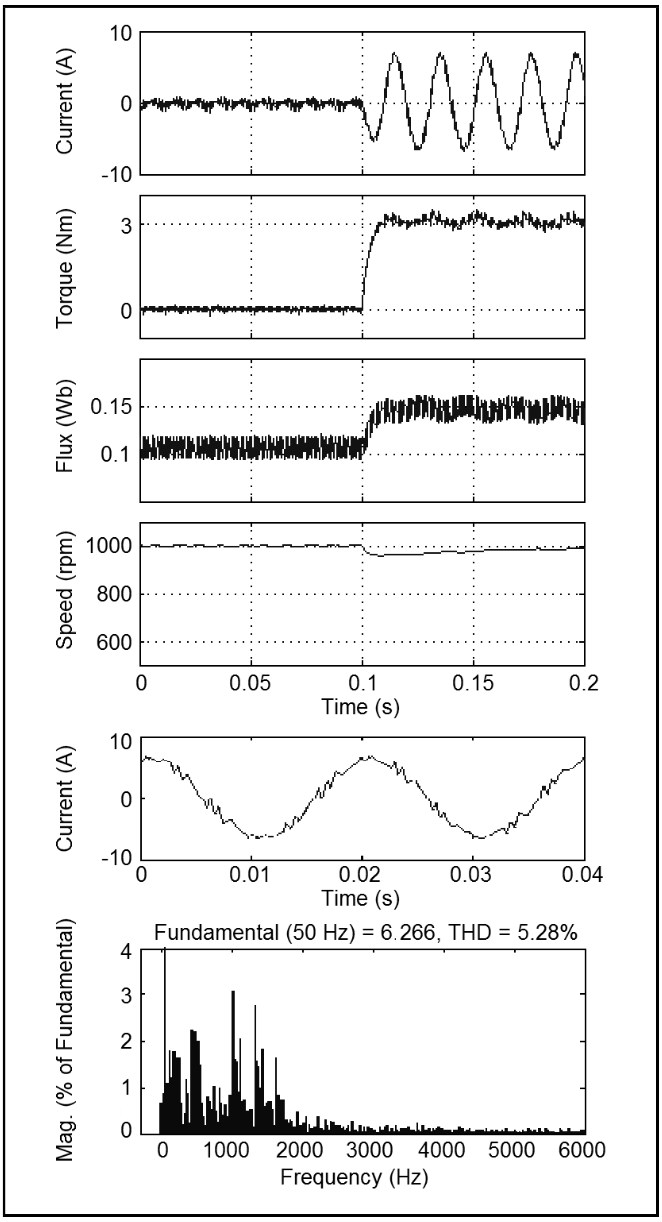

Figure 7. Response of DTC method 4 at 1000 rpm with an external load of 3 Nm.

Table 2. Quantitative comparison of the proposed DTC methods with existing DTC methods.

Method	f_{av} (Hz)	ϕ_{ripple} (Wb)	T_{ripple} (Nm)	*% THD* of Stator Current
Classical DTC	5.36 k	0.0066	0.2004	6.73%
Y. Zhang and J. Zhu[13]	4.41 k	0.0043	0.1222	5.85%
Y. Zhang and J. Zhu[14]	3.22 k	0.0017	0.1110	4.67%
Proposed DTC method 1	4.99 k	0.0064	0.1956	6.97%
Proposed DTC method 2	4.68 k	0.0063	0.1563	5.70%
Proposed DTC method 3	1.63 k	0.0048	0.1092	4.40%
Proposed DTC method 4	3.09 k	0.0086	0.1107	5.28%

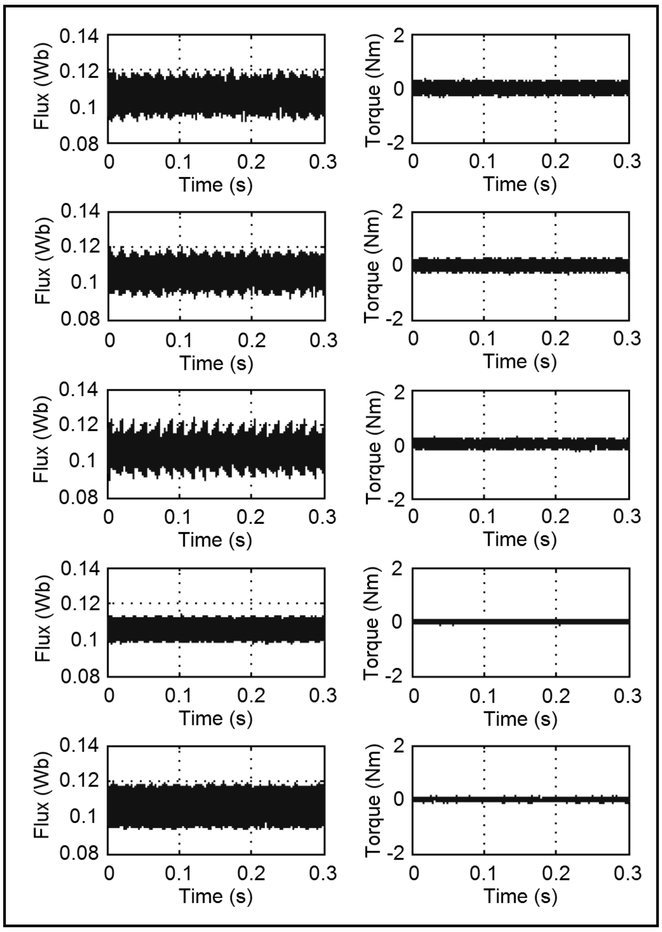

Figure 8. Steady state response at 200 rpm (10% of the rated speed) for classical DTC, DTC method 1, DTC method 2, DTC method 3, and DTC method 4.

in the view of stator current THD. The dominant harmonics between 2000 Hz and 3000 Hz in the proposed DTC method 3 are much lesser than as compared to the other proposed methods and classical DTC method.

The average commutation frequency is calculated using the formula, $f_{av} = N/K/0.05$, where, N is the total commutation instants of all the legs of the inverter used in the DTC methods during fixed period (e.g., 0.05 s in this paper), and K is the switch numbers.

The Root Mean Square (RMS) torque ripple is calculated for all the DTC methods in this paper. The proposed DTC method 3 exhibits its better performance in terms of torque ripple, stator current THD, and average commutation frequency, f_{av}. The DTC method 3 exhibits better performance while comparing all other proposed methods and the classical DTC method.

The average commutation frequency of the proposed DTC method 3 is 1.63 kHz. The proposed DTC method 3 has its average commutation frequency, f_{av} only 51% and 37% of that of existing DTC methods available in the literature Zhang and Zhu[13] and Zhang and Zhu,[14] respectively. This validates the superiority of the proposed DTC methods. The DTC method 4 provides lesser average commutation frequency as compared to Zhang and Zhu[13] whereas torque ripple is less when compared to both considered publications.[13,14]

Table 2 also informs us that all the proposed DTC methods produce lesser torque ripple as compared to the classical DTC method. While comparing the existing DTC methods of Zhang and Zhu,[13,14] the proposed DTC method 3 provides lesser torque ripple. The proposed DTC method 3 gives torque ripple only 54%, 89%, 98% of that of the classical DTC method, Zhang and Zhu,[13] and Zhang and Zhu,[14] respectively. The DTC method 4 exhibits lesser torque ripple as compared to classical DTC, Zhang and Zhu works,[13,14] DTC method 1, and DTC method 2. In terms of average commutation frequency, torque ripple and THD of stator current, the DTC method 3 shows better performance among all the DTC methods.

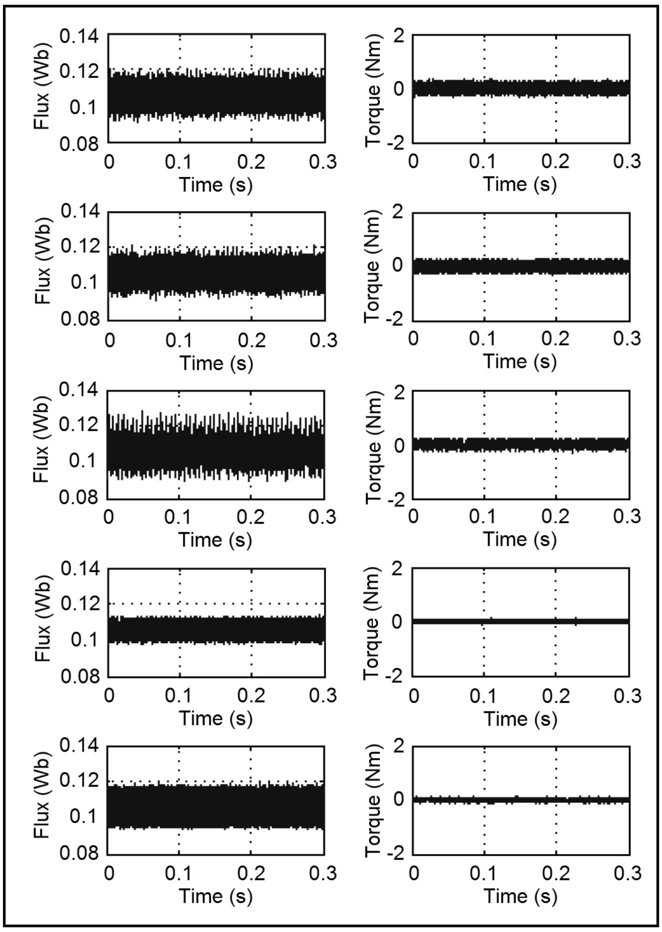

Figure 9. Steady state response at 500 rpm (25% of the rated speed) for classical DTC, DTC method 1, DTC method 2, DTC method 3, and DTC method 4.

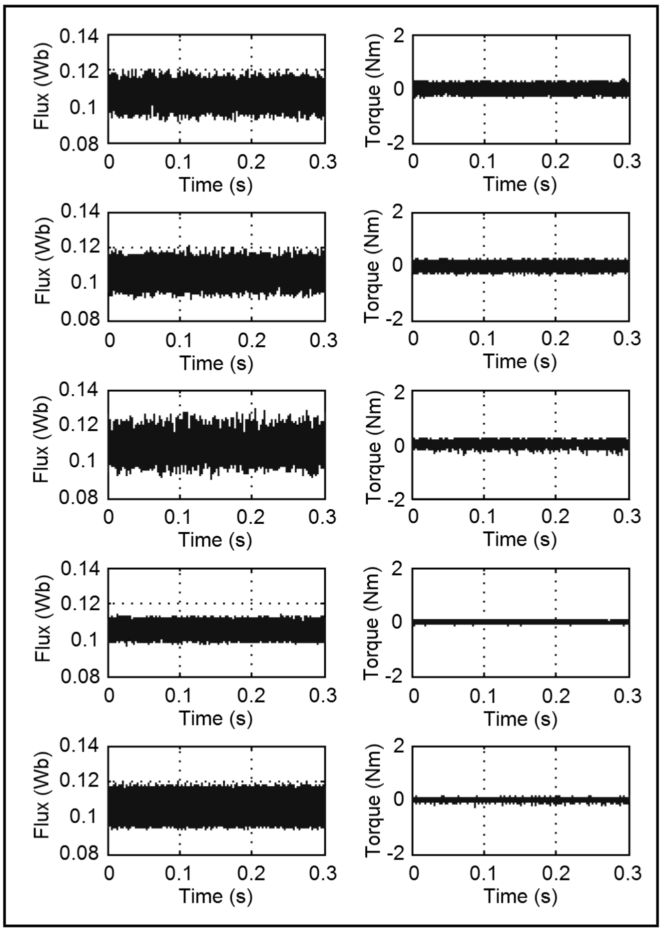

Figure 10. Steady state response at 1000 rpm (50% of the rated speed) for classical DTC, DTC method 1, DTC method 2, DTC method 3, and DTC method 4.

5.2. Results at 10% of Rated Speed

The proposed DTC method is analysed at different operating points. In Fig. 8, the operating point is considered at 200 rpm (10% of the rated speed) without load as an example. Figure 8 shows the flux and torque responses for classical DTC, DTC method 1, DTC method 2, DTC method 3, and DTC method 4, respectively. From top to bottom, the responses shown in Fig. 8 are classical DTC, DTC method 1, DTC method 2, DTC method 3 and DTC method 4, respectively, the flux response is in the left, and the torque response is in the right.

It is seen that at the operating point at 200 rpm, the DTC method 1 gives almost the same performance as compared to classical DTC because their switching pattern is almost similar. However the DTC method 2 gives lesser torque ripple as compared to classical DTC and DTC method 1, but it gives instantaneous spikes in flux. The main drawback of the DTC drive is more torque ripple at lower speed. So this analysis provides an important conclusion: DTC method 3 presents the best overall performance among the four kinds of proposed DTC methods and classical DTC.

5.3. Results at 25% of Rated Speed

At this operating point, in the view of the flux and torque ripple, the DTC method 3 exhibits better performance followed by DTC method 4, DTC method 2, DTC method 1, and classical DTC. The ripples in the flux and torque waveform also significantly diminished in the DTC method 3 as compared to the other methods proposed in this paper. This can be observed from Fig. 9.

5.4. Results at 50% of Rated Speed

As is shown in Fig. 10, the high ripples and distortion in the flux and torque waveforms can be noticed in all the methods.

However, a remarkable reduction in torque ripple can be observed in DTC method 3. DTC method 3 and DTC method 4 provide almost similar torque ripple, but the instantaneous spikes are noticed in torque response of DTC method 4.

5.5. Results at 75% of Rated Speed

DTC method 1 almost imitates the classical DTC. DTC method 2 presents the lower torque ripple among the other methods. According to the switching table of this method, at any point of time, the inverter will provide half voltages for two lines and zero voltage for one line. This voltage is not sufficient to rotate the rotor at this speed. The DTC method 3 gives satisfactory operation up to 70% of the rated speed. However, the DTC method 4 provides lesser torque ripple compared to all other methods.

5.6. Results at 100% of Rated Speed

It is found that there is no significant improvement in the DTC method 1 as compared to classical DTC. Large vectors are considered in classical DTC and DTC method 1. According to Eq. (13), this will lead large torque ripples. At the same

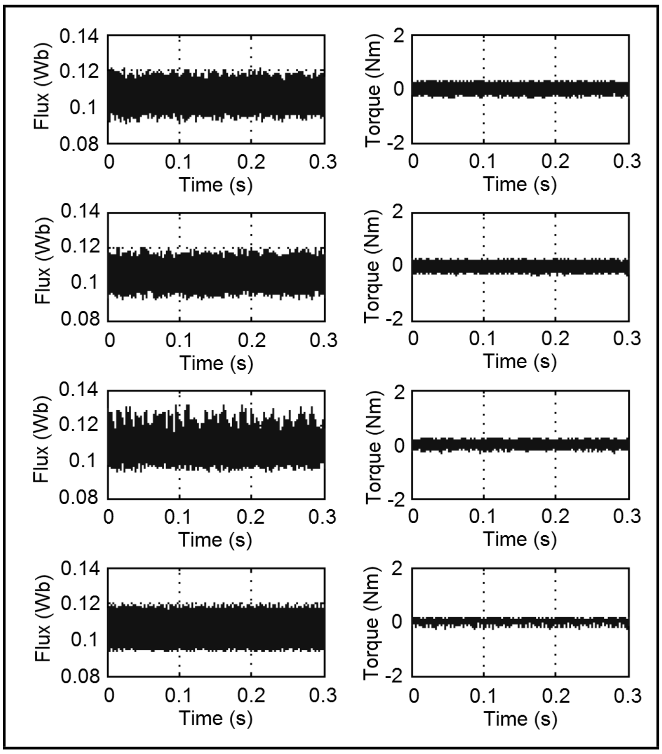

Figure 11. Steady state response at 1500 rpm (75% of the rated speed) for classical DTC, DTC method 1, DTC method 2, and DTC method 4.

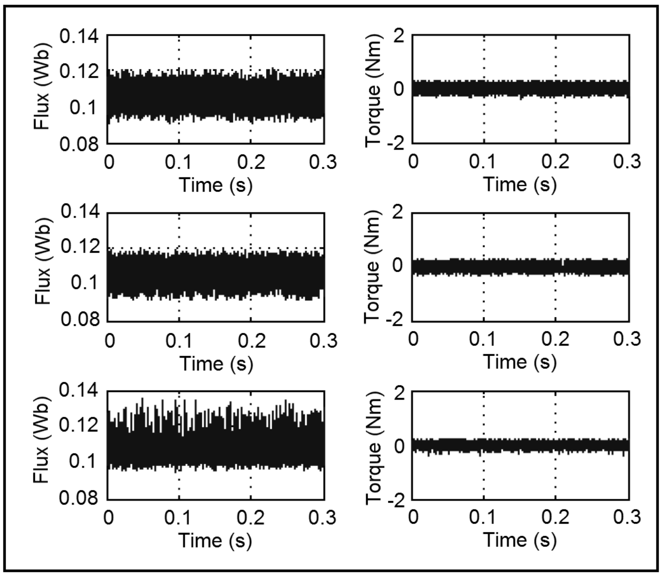

Figure 12. Steady state response at 2000 rpm (100% of the rated speed) for classical DTC, DTC method 1, and DTC method 2.

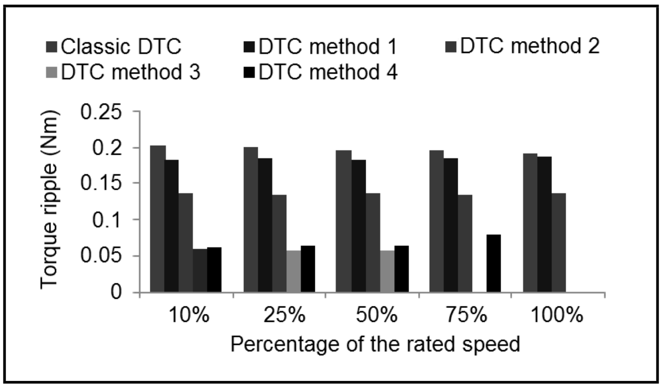

Figure 13. Comparison of the torque ripple for classical DTC, DTC method 1, DTC method 2, DTC method 3, and DTC method 4.

time, the DTC method 2 presents lesser torque ripples as compared to other methods. Nevertheless, the DTC method 3 is not able to trace the reference target. It can be seen from Fig. 13, all the proposed DTC methods provide lesser torque ripple at different operating point compared to classical DTC method.

5.7. Responses to External Load Disturbance

The responses to the external disturbances are shown in Fig. 14(a) through Fig. 14(e) for classical DTC, DTC method 1, DTC method 2, DTC method 3, and DTC method 4, respectively. The motor is operated at a steady state with 2.5 Nm and 50% of the rated speed, and then the load is suddenly removed in order to check the disturbance rejection capability of the classical and proposed DTC methods.

In a very short period, the motor speed returns to its original speed due to its fast torque response. It is observed that about 3% peak speed increases for all the proposed DTC methods 1, 2, 3 and 4, whereas it is about 2.5% for the classical DTC method when the load is suddenly removed. However, almost all the DTC methods including the classical DTC method take the same time to reach their original speed after the load is removed. This comparison informs that all the proposed DTC methods exhibit their fast response of torque as compared to classical DTC. Even though the peak speed increases about 3%, it takes lesser time to reach its steady state, whereas the classical DTC takes same time to reach from its 2.5% peak speed. However the classical DTC, DTC method 1, and DTC method 2 exhibit the best performance at the cost of larger torque ripple, whereas DTC method 3 provides lesser torque ripple and better performance in terms of disturbance rejection.

5.8. Harmonics and Mechanical Vibration Reduction

The major disadvantages of the DTC based PMSM drive is more torque ripple, and that leads to mechanical vibrations and acoustic noise. For electric and hybrid vehicle applications, the torque ripple could result in mechanical vibration and acoustic noise. These phenomena are undesirable for most of the applications. In this paper, the status of the Total Harmonic Distortion in the current waveform, RMS level of vibration, and noise has been examined, and their comparison is shown in Fig. 15. The RMS level of the vibration is calculated using LabVIEW software. This proves that the proposed DTC method is able to suppress the torque ripple and mechanical vibration.

6. IMPORTANT OBSERVATIONS

In this paper, the classical DTC method and all the proposed DTC methods are comparatively investigated in the aspect of torque ripple, disturbance rejection performance during external load disturbance, and mechanical vibration. From the results indicated earlier, it is found that the torque ripple in the proposed DTC methods is less as compared to the classical DTC method and existing literatures. In most of the oper-

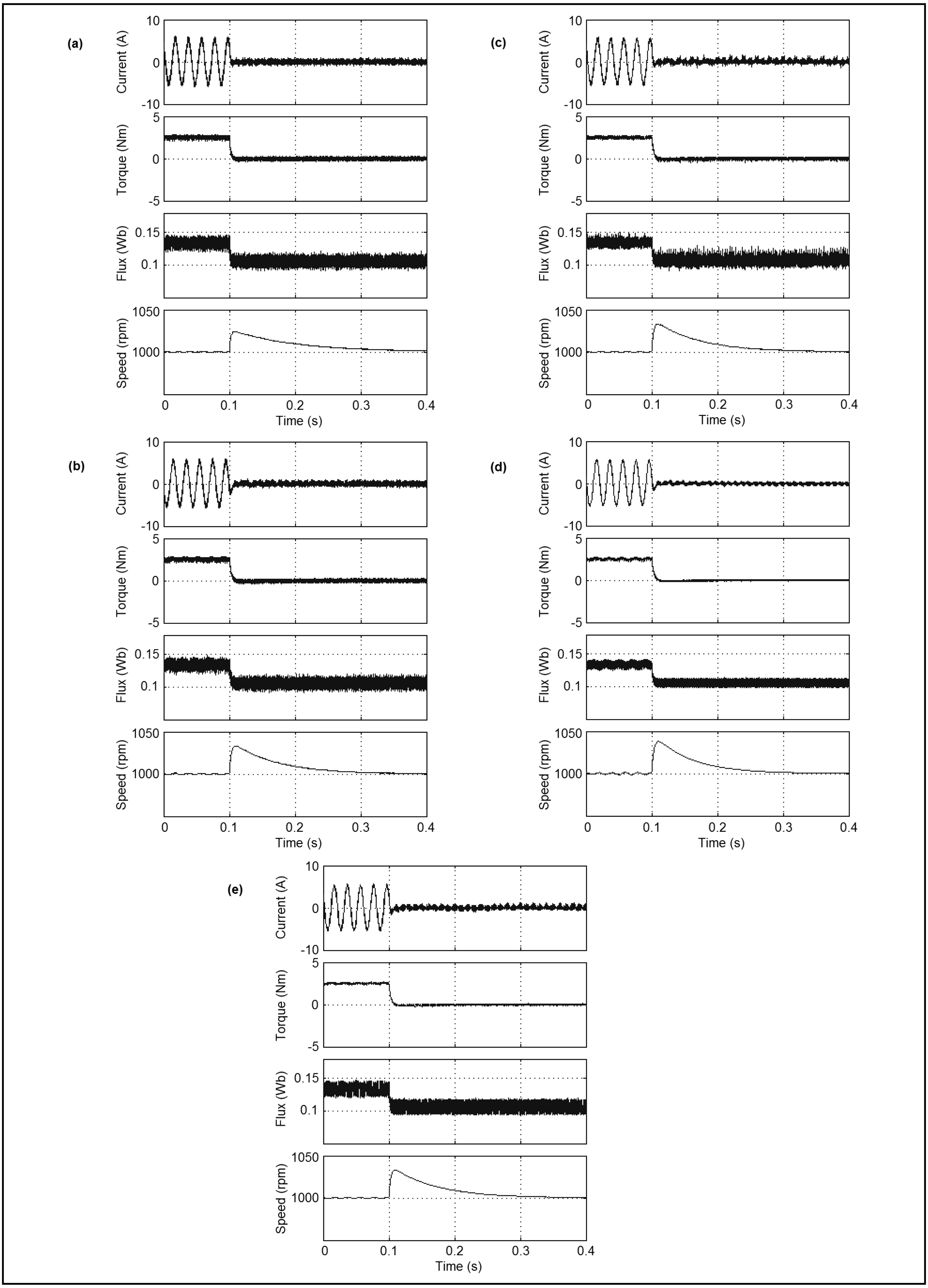

Figure 14. Response to external load disturbance for: (a) Classical DTC; (b) DTC method 1; (c) DTC method 2; (d) DTC method 3; (e) DTC method 4.

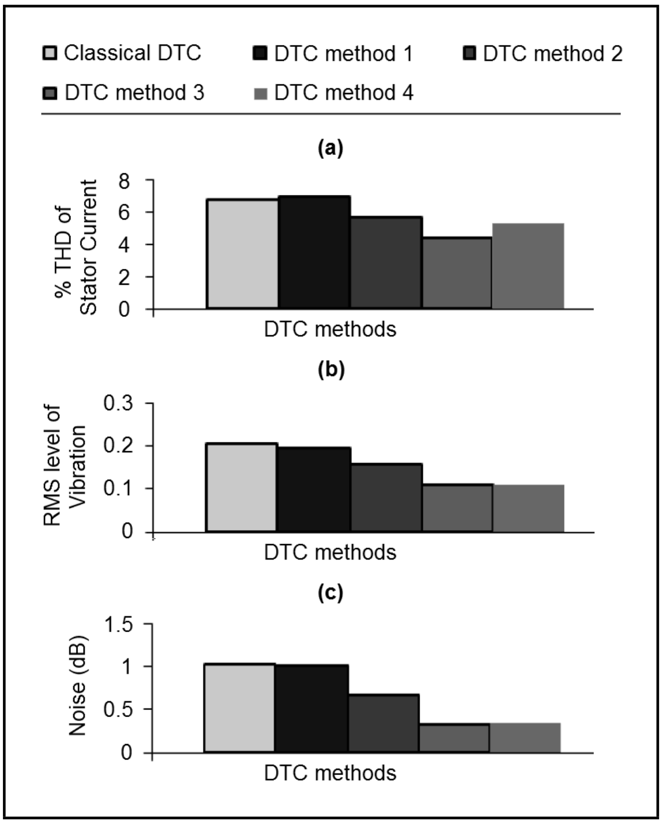

Figure 15. Response of DTC methods in the view of Mechanical Vibration: (a) Percentage THD of Stator Current; (b) RMS level of Vibration; (c) Noise produced in various DTC methods.

ating points, the proposed DTC method 1 provides slightly higher torque ripple as compared to proposed DTC methods 2, 3, and 4. However, proposed DTC method 3 shows better performance in terms of torque ripple as compared to the classical DTC method and proposed DTC methods 1, 2, and 4. The usage of small and zero voltage vectors in proposed DTC method 3 provide better performance with the comparison of all the methods including the classical DTC method. Once again, all the DTC methods exhibit almost similar decelerating capability; however, the proposed DTC method 3 provides lesser ripple in the current waveform. All the proposed and existing DTC methods show good disturbance rejection characteristics at the cost of higher torque ripple except proposed DTC method 3. In the view of mechanical vibration, all the proposed DTC methods provide lesser vibration as compared to the classical DTC method.

7. CONCLUSIONS

In this paper, a simple method to minimize the torque ripple for a DTC of PMSM drives have been proposed. The new switching table is proposed in which only any two voltage vectors (LZ, MZ, and SZ) are utilized out of four voltage vectors (L, M, S, Z) available due to the increment in the level of inverter. The performance of the proposed DTC method is comparatively investigated with the classical DTC and existing literatures. The simulation results prove that the proposed DTC methods able to diminish the torque ripple at different operating points as compared to the classical DTC. Consequently, the proposed DTC method also gives satisfactory performance during external load disturbance operations. The proposed DTC method is also capable of suppressing mechanical vibration and noise. The settling time of the torque can be reduced if compared with the classical DTC method, furthermore, the related current ripple is also reduced. The proposed DTC methods also retain the merits of simplicity and robustness as in DTC.

REFERENCES

[1] Blaschke, F. The principle of field orientation as applied to the new TRANSVECTOR closed loop control system for rotating field machines, *Siemens Review*, **34**, 217–220, (1972).

[2] Takahashi, I. and Nogushi, T. A new quick-response and high-efficiency control strategy of an induction motor, *IEEE Transactions on Industry Applications*, **IA-22** (5), 820–827, (1986).

[3] Depenbrock, M. Direct self-control (DSC) of inverter-fed induction machine, *IEEE Transactions on Power Electronics*, **3** (4), 420–429, (1988).

[4] Zhong, L., Rahman, M. F., Hu, W., and Lim, K. Analysis of direct torque control in permanent magnet synchronous motor drives, *IEEE Transactions on Power Electronics*, **12** (3), 528–536, (1997).

[5] Morales-Caporal, R. and Pacas, M. Encoderless predictive direct torque control for synchronous reluctance machines at very low and zero speed, *IEEE Transactions on Industrial Electronics*, **55** (12), 4408–4416, (2008).

[6] Kang, J. K. and Sul, S. K. New direct torque control of induction motor for minimum torque ripple and constant switching frequency, *IEEE Transactions on Industry Applications*, **35** (5), 1076–1082, (1999).

[7] Buja, G. S. and Kazmierkowski, M. P. Direct torque control of PWM inverter-fed AC motors—A survey, *IEEE Transactions on Industrial Electronics*, **51** (4), 744–757, (2004).

[8] Abad, G., Rodriguez, M. A., and Poza, J. Two-level VSC based predictive direct torque control of the doubly fed induction machine with reduced torque and flux ripples at low constant switching frequency, *IEEE Transactions on Power Electronics*, **23** (3), 1050–1061, (2008).

[9] Foo, G. and Rahman, M. F. Sensorless direct torque and flux-controlled IPM synchronous motor drive at very low speed without signal injection, *IEEE Transactions on Industrial Electronics*, **57** (1), 395–403, (2010).

[10] Foo, G. and Rahman, M. F. Sensorless sliding-mode MTPA control of an IPM synchronous motor drive using a sliding-mode observer and HF signal injection, *IEEE Transactions on Industrial Electronics*, **57** (4), 1270–1278, (2010).

[11] Lee, K. B. and Blaabjerg, F. An improved DTC-SVM method for sensorless matrix converter drives using an overmodulation strategy and a simple nonlinearity compensation, *IEEE Transactions on Industrial Electronics*, **54** (6), 3155–3166, (2007).

[12] Andreescu, G. D., Pitic, C., Blaabjerg, F., and Boldea, I. Combined flux observer with signal injection enhancement for wide speed range sensorless direct torque control of IPMSM drives, *IEEE Transactions on Energy Conversion*, **23** (2), 393–402, (2008).

[13] Zhang, Y. and Zhu, J. Direct torque control of permanent magnet synchronous motor with reduced torque ripple and commutation frequency, *IEEE Transactions on Power Electronics*, **26** (1), 235–248, (2011).

[14] Zhang, Y. and Zhu, J. A Novel Duty Cycle Control Strategy to Reduce Both Torque and Flux Ripples for DTC of Permanent Magnet Synchronous Motor Drives with Switching Frequency Reduction, *IEEE Transactions on Power Electronics*, **26** (10), 3055–3067, (2011).

[15] Zhang, Y., Zhu, J., Xu, W., and Guo, Y. A simple method to reduce torque ripple in direct torque-controlled permanent-magnet synchronous motor by using vectors with variable amplitude and angle, *IEEE Transactions on Industrial Electronics*, **58** (7), 2848–2859, (2011).

[16] Zhang, Y., Zhu, J., Zhao, Z., Xu, W., and Drroell, D. G. An improved direct torque control for three-level inverter-fed induction motor sensorless drive, *IEEE Transactions on Power Electronics*, **26** (7), (2011).

[17] Sivaprakasam, A. and Manigandan, T. Combined Effect of Fuzzy Logic Controller and Optimized Voltage Vector in Torque Ripple Reduction of Direct Torque Controlled Permanent Magnet Synchronous Motor, *World Journal of Modelling and Simulation*, **10** (2), 92–107, (2014).

[18] Zhang, Y., Zhu, J., and Xu, W. Predictive torque control of permanent magnet synchronous motor drive with reduced switching frequency, *Proc. of 2010 International Conference on Electrical Machines and Systems*, 798–803, (2010).

[19] Adhavan, B. and Jagannathan, V. Performance comparison of hysteresis pulse width modulation and space vector pulse width modulation techniques for torque ripple reduction in permanent magnet synchronous motor using iterative learning control, *Journal of Vibration and Control*, **20** (5), 698–712, (2014).

[20] Casadei, D., Profumo, F., Serra, G., and Tani, A. FOC and DTC: Two viable schemes for induction motors torque control, *IEEE Transactions on Power Electronics*, **17** (5), 779–787, (2002).

[21] Cheng, B. and Tesch, T. R. Torque feed forward control technique for permanent-magnet synchronous motors, *IEEE Transactions on Industrial Electronics*, **57** (3), 969–974, (2010).

[22] Flach, E., Hoffmann, R., and Mutschler, P. Direct mean torque control of an induction motor, *Proc. of the 7th European Conference on Power Electronics and Applications EPE'97*, **3**, 672–677, (1997).

[23] Gulez, K., Adam A. A., and Pastaci H. Torque Ripple and EMI Noise Minimization in PMSM Using Active Filter Topology and Field-Oriented Control, *IEEE Transactions on Industrial Electronics*, **55** (1), 251–257, (2008).

[24] Kouro, S., Bernal, R., Miranda, H., Silva, C., and Rodriguez, J. High performance torque and flux control for multilevel inverter fed induction motors, *IEEE Transactions on Power Electronics*, **22** (6), 2116–2123, (2007).

[25] Ortega, C., Arias, A., Caruana, C., Balcells, J., and Asher, G. M. Improved waveform quality in the direct torque control of matrix-converter-fed PMSM drives, *IEEE Transactions on Industrial Electronics*, **57** (6), 2101–2110, (2010).

[26] Pacas, M. and Weber, J. Predictive direct torque control for the PM synchronous machine, *IEEE Transactions on Industrial Electronics*, **52** (5), 1350–1356, (2005).

[27] Romeral, L., Arias, A., Aldabas, E., and Jayne, M. Novel direct torque control (DTC) scheme with fuzzy adaptive torque-ripple reduction, *IEEE Transactions on Industrial Electronics*, **50** (3), 487–492, (2003).

[28] Shyu, K. K., Lin, J. K., Pham, V. T., Yang, M. J., and Wang, T. W. Global minimum torque ripple design for direct torque control of induction motor drives, *IEEE Transactions on Industrial Electronics*, **57** (9), 3148–3156, (2010).

[29] Tang, L., Zhong, L., Rahman, M. F., and Hu, Y. A novel direct torque controlled interior permanent magnet synchronous machine drive with low ripple in flux and torque and fixed switching frequency, *IEEE Transactions on Power Electronics*, **19** (2), 346–354, (2004).

[30] Tursini, M., Chiricozzi, E., and Petrella, R. Feed forward flux-weakening control of surface-mounted permanent-magnet synchronous motors accounting for resistive voltage drop, *IEEE Transactions on Industrial Electronics*, **57** (1), 440–448, (2010).